

# Estimations of Vapor Pressures by Thermogravimetric Analysis of the Insensitive Munitions IMX-101, IMX-104, and Individual Components

Michael F. Cuddy,<sup>\*,[a]</sup> Aimee R. Poda,<sup>[a]</sup> and Mark A. Chappell<sup>[a]</sup>

**Abstract:** We have calculated the vapor pressures of the new explosives ordnances IMX-101 and IMX-104 and their respective components, 2,4-dinitroanisoie (DNAN), nitroguanidine (NQ), nitrotriazolone (NTO), and hexahydro-1,3,5-trinitro-1,3,5-triazine (RDX) by the method of rising temperature thermogravimetric analysis. Clausius-Clapeyron relationships were assumed for each case and the vapor pressures were estimated from the Langmuir equation over an appropriate temperature range just below substance melting/decomposition points. For vapor pressures extrapolated to room temperature, the rank with respect to decreasing volatility was found to be: DNAN > IMX-104 > IMX-101 > NQ > RDX > NTO. Interestingly, vapor pressure depression is

observed in IMX formulations, where the formulation has a lower vapor pressure than its most volatile component, DNAN. The enthalpy of sublimation was determined for each substance and formulation from Clausius-Clapeyron equations generated by analysis of the thermogravimetric data. The general trends in vapor pressures and sublimation enthalpies associated with the component materials were in good agreement with previous experimental and computational results. The results obtained by this study have importance for future investigations of IMX, specifically for chemical detection and assessment of environmental fate.

**Keywords:** IMX-101 • IMX-104 • Vapor pressure • Langmuir equation • Clausius-Clapeyron

## 1 Introduction

Vapor pressure is a fundamental property that provides a critical means to assess the potential for environmental mobility of a material as part of a comprehensive life cycle assessment of overall environmental impact. Vapor pressure is also one key contributing factor in fugacity models to simulate the complex behavior of chemicals in the environment [1]. For energetic materials such as explosives, knowledge of vapor pressures is crucial for designing sensors capable of detecting the generally trace quantities of vapor associated with a particular explosive [2]. For new and emerging explosives formulations, the determination of vapor pressure represents an important step in expediently and efficiently assessing the environmental fate and transport phenomena associated with the material [3].

The United States Army recently approved a new class of insensitive, melt-cast munitions developed under the Common Low-Cost Insensitive Munitions Explosives (CLIMEx) program that exhibit superior shock resistance compared to conventional explosives such as TNT. Given the designation of IMX, these formulations are expected to supplant TNT for Army ordnance in the near future. Consequently, it is imperative to have information on physical properties of these formulations, such as vapor pressure, in order to assess the possible environmental impacts and to determine appropriate means for vapor detection. IMX-101

and IMX-104 are the two major formulations of this class of materials, and are comprised of the nitrated chemicals DNAN, NTO, NQ, and RDX. Few studies exist that explicitly evaluate vapor pressures for each discrete component, and none, to the best of our knowledge, have comprehensively investigated the combined effect of these materials in the IMX formulations. Recently, estimations of vapor pressures have been carried out for individual constituents and other explosives in a variety of experimental and computational methods [4–6].

Approaches to measure vapor pressures for solid materials experimentally generally rely on estimations based upon the Clausius-Clapeyron relationship. Two related thermogravimetric analysis (TGA) methods include the rising temperature method and the isothermal TGA method, which have been employed to estimate vapor pressures for explosives and other organic substances [7,8]. Other methods for determining vapor pressure include manometry [9],

[a] M. F. Cuddy, A. R. Poda, M. A. Chappell  
Environmental Laboratory  
US Army Corps of Engineer Research and Development Center  
3909 Halls Ferry Rd.  
Vicksburg, MS, 39180, USA  
\*e-mail: michael.cuddy@usace.army.mil

transpiration [10], and gas chromatography [11]. The former methods require stringent vacuum conditions and precise pressure measurement, whereas the latter (chromatographic) methods yield vapor pressures representative of supercooled liquid phases for substances that are crystalline solids at room temperature [11]. Thus, we have chosen TGA as the most effective means to estimate vapor pressures for IMX formulations, based on the versatility, accessibility and simplicity of the technique. Herein, we have measured rising temperature thermogravimetric (TG) mass loss for IMX-101 and IMX-104 and each major constituent compound for the two formulations and have calculated vapor pressures based upon the Langmuir equation. Ultimately, the understanding achieved by investigations of fundamental physical properties for IMX lends critical insight to the environmental implications and analytical detection of these new formulations.

## 2 Experimental Section

A list of the components associated with the IM formulations IMX-101 and IMX-104 investigated in this work along with their melting points and molecular weights is provided in Table 1. DNAN (Alfa Aesar, 98%), NTO (BAE Systems, Batch # NTO 0-13), NQ (Aldrich, with 25% H<sub>2</sub>O), and RDX (Holston Army Ammunition Plant, Kingsport, TN) were used as received without further purification or modification. IMX melt-cast formulations (Holston Army Ammunition Plant, Kingsport, TN) were also used as received. Each formulation contains trace quantities of unidentified binder material. For practicality, only the fine fractions (< 500 μm) of the IMX formulations were selected for thermal analyses.

Simultaneous TG and differential scanning calorimetry (DSC) measurements were performed in a SiC furnace with a Netzsch STA 449 F1 Jupiter instrument with automated sample changer. Samples were loaded in alumina crucibles such that the bottoms of each 6 mm diameter pan were

just covered (typically amounting to ca. 10 mg material). For analysis by the rising temperature method, samples were heated from 55 to 600 °C at 10 °C min<sup>-1</sup>. Benzoic acid (Sigma-Aldrich, >99.5%) was used for instrument calibration. Analyses were performed under 20 mL min<sup>-1</sup> protective nitrogen flow and with 70 mL min<sup>-1</sup> nitrogen purge to inhibit combustion. Multiple measurements were made for each explosive substance and for benzoic acid.

## 3 Results and Discussion

Irving Langmuir first introduced an equation to describe the phenomena associated with vapor pressure of metallic tungsten [16], which is modified here for applicability to estimation of vapor pressures extracted from thermogravimetry data:

$$p_i = \left( \frac{dm}{dt} \right)_i \sqrt{\frac{T_i}{M}} \left( \frac{A\sqrt{2\pi R}}{\alpha} \right) \quad (1)$$

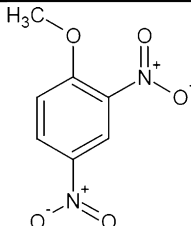
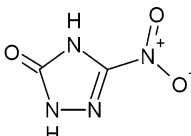
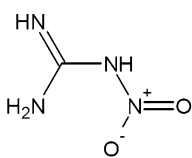
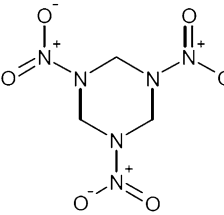
In Equation (1),  $p_i$  denotes vapor pressure at temperature  $T_i$  given the time-dependent (and hence temperature-dependent) mass change,  $(dm/dt)_i$ ,  $M$  represents the gas-phase molecular weight of the species of interest,  $A$  is the inverse of the exposed surface area of the material,  $R$  is the ideal gas constant, and  $\alpha$  is the vaporization coefficient. For simplification, we define the variables  $v_i$  and  $k$  [7],

$$v_i = A (dm/dt)_i \sqrt{T_i/M} \quad (2)$$

$$k = \sqrt{2\pi R}/\alpha \quad (3)$$

Under vacuum conditions,  $\alpha$  is unity and may be disregarded in the equation. However, for TGA under flowing gas conditions,  $\alpha$  must be determined explicitly [17].

**Table 1.** IMX-101 and IMX-104 formulation components.

	DNAN	NTO	NQ	RDX
Structure				
Chemical name	2,4-dinitroanisole	5-nitro-1,2,4-triazol-3-one	nitroguanidine	1,3,5-trinitro-1,3,5-triazine
MW [g mol <sup>-1</sup> ]	198.1	130.1	104.1	222.1
Melting point [°C]	86–95 <sup>a)</sup>	262 <sup>b)</sup>	232–240 <sup>c)</sup>	205 <sup>d)</sup>
IMX-101	✓	✓	✓	
IMX-104	✓	✓		✓

a) From Ref. [12]. b) From Ref. [13]. c) From Ref. [14]. d) From Ref. [15].

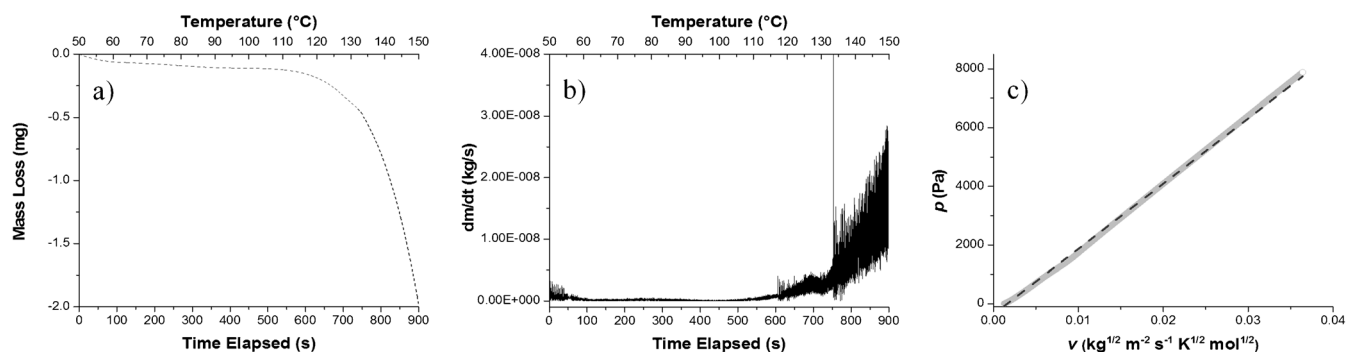


**Figure 1.** Benzoic acid method used to determine the instrument calibration factor  $k$ . Mass loss as a function of time and temperature as measured by the instrument is plotted in (a). This raw data is transformed by point differentiation to generate the plot shown in (b). Finally, these data are transformed to  $v$  and plotted with pressure,  $p$ , calculated from the Antoine expression for benzoic acid, (c). A best-fit line to the data yields a slope,  $k$  of  $2.224 \times 10^5 \text{ J}^{1/2} \text{ mol}^{-1/2} \text{ K}^{-1/2}$  ( $R^2 > 0.99$ ).

Benzoic acid was employed as the model material for determination of  $k$  (and by association,  $\alpha$ ) because it is well characterized and has been used extensively for such experiments [7, 18, 19]. A reduced Antoine expression describing the relationship between pressure (in Pa) and temperature for benzoic acid just below its melting point (122 °C) is given in Equation (4) [7, 20].

$$\ln(p_i) = 34.146 - 10831/T_i \quad (4)$$

Using this relationship, a Matlab script was prepared to handle corresponding TG data and determine  $\alpha$ . Mass loss determined by thermogravimetry measurements (Figure 1a) was point-differentiated by the method of secant approximation to generate  $(dm/dt)_i$  (Figure 1b). From these values, Equation (2) was solved for  $v_i$  as a function of  $T_i$ . A plot of  $p_i$  from Equation (4), vs.  $v_i$ , yielded a best-fit slope,  $k$ , of  $2.224 \times 10^5 \text{ J}^{1/2} \text{ mol}^{-1/2} \text{ K}^{-1/2}$ , (Figure 1c). This instrument correction parameter, containing the vaporization coefficient  $\alpha$ , was used in all subsequent analyses.

The components of the IMX formulations (Table 1) were investigated individually and independently to determine respective vapor pressures. Raw TG and DSC data for each component are shown in Figure 2a–d. Generally, the TG traces indicate that each substance undergoes only one significant mass loss event that coincides with a phase change in the DSC (positive values denote exothermic events). In each case save DNAN, a sharp exotherm is observed at the point of greatest rate of mass loss. These exothermic events are likely due to exothermic decomposition that dominates competitive endothermic vaporization processes. Indeed, Long et al. observed similar phenomena for RDX at temperatures slightly above its melting point [21], and likewise attributed the exothermic peak to decomposition. For DNAN, characteristic endothermic events are observed: melting at 91 °C and boiling commencing at 205 °C. Because two phase changes were observed for DNAN in the TG/DSC analyses, we have calculated the vapor pressure of both crystalline and liquid DNAN. Mass loss and

DSC data provided for IMX-101 and 104 in Figure 3a and c indicate that the formulations behave as a collective of their discrete components. In particular, the DSC traces for each IMX formulation appear to be superpositions of the individual chemicals in the blend. There appears to be little influence in the thermal properties of the formulations by either binders or the melt-cast process that is employed to develop the IMX. Based on TG measurements, decomposition of the IMX formulations commences just below 200 °C.

Raw TG data for IMX and its components were handled with a Matlab script similar to that used for benzoic acid instrument calibration. However, instead of generating plots of  $p_i$  vs.  $v_i$ , Clausius-Clapeyron relationships were assumed and corresponding values for  $\ln(p_i)$  were plotted against inverse temperature over an appropriate range in which the relationship remained linear. The  $T$  range of linearity is provided for each substance in Table 2, along with the corresponding best-fit function. In addition, the raw data and fits are plotted together in Figure 2e for the IMX components. It is evident from this plot that the vapor pressure of DNAN in particular far exceeds the vapor pressure of any of the other components. Indeed, if the Clausius-Clapeyron relationship is extended to  $T = 298 \text{ K}$  for each substance, the vapor pressures rank as DNAN > NQ > RDX > NTO (excluding liquid DNAN).

Brady and co-workers recently demonstrated a similar TGA-based technique to estimate, among others, the vapor pressures of NTO and RDX [7]. They determined that, if extrapolated to 298 K, the vapor pressure of NTO and RDX were equivalent ( $2.10 \times 10^{-6} \text{ Pa}$ ), whereas other literature sources they cited reported vapor pressures ranging from  $10^{-7}$ – $10^{-9} \text{ Pa}$  for RDX and  $10^{-7} \text{ Pa}$  for NTO [8, 22, 23]. Notably, these values are also significantly different from those calculated in our work (on the order of  $10^{-8} \text{ Pa}$ ). The ostensible reason for disagreement among many sources is that the extrapolated vapor pressure at room temperature suffers from deviation from linearity over a wide temperature range. Thus, small variations in Clausius-Clapeyron relations manifest in large differences once extrapolated to extrema such as

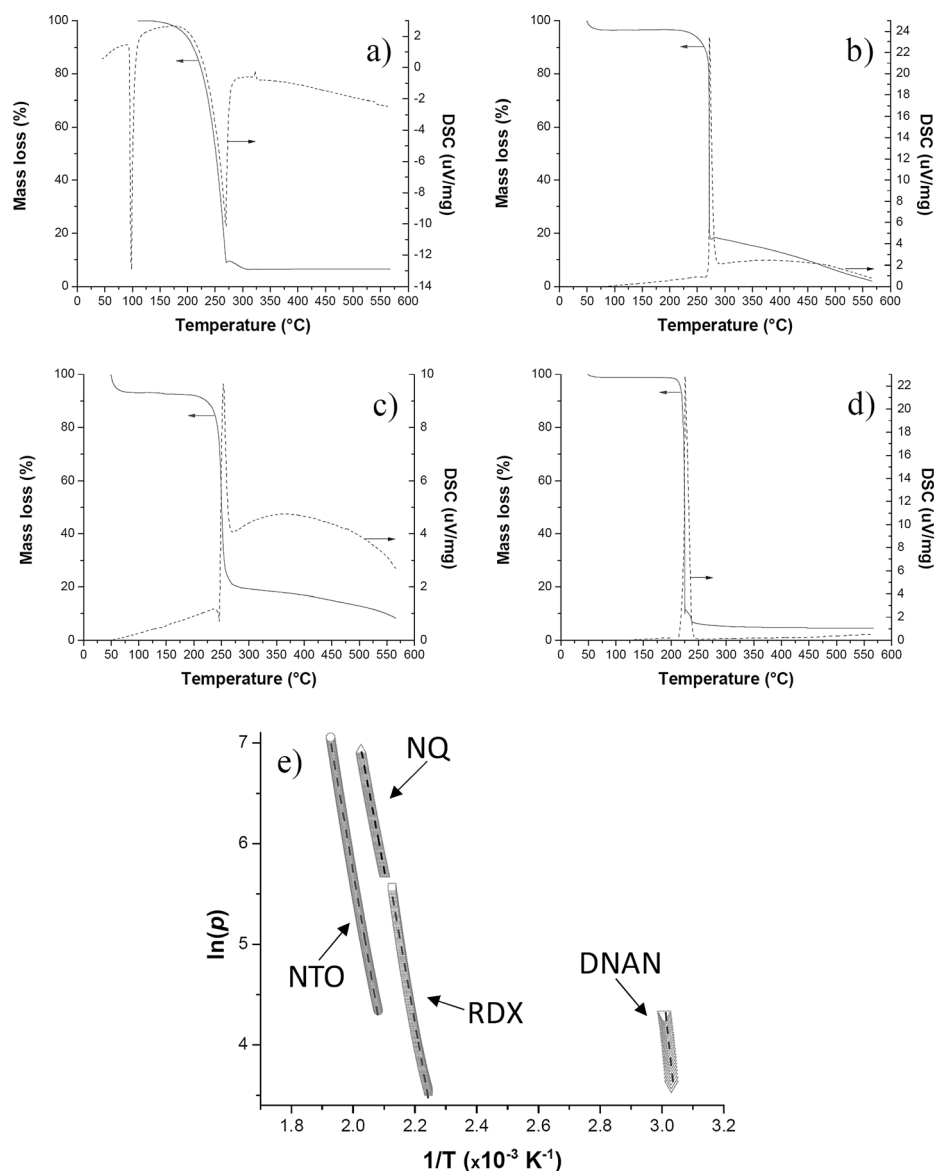


**Figure 2.** Mass loss (left y axes) and DSC traces (right y axes) for (a) DNAN (solid), (b) NTO, (c) NQ, and (d) RDX. (e) Raw TG data are converted to plots of  $\ln(p)$  vs.  $1/T$  for temperatures just below the material melting point. Linear regression analyses of each data set are provided as best-fit dashed lines (all with  $R^2 \geq 0.99$ ). A plot for liquid DNAN is omitted because it overlaps with several of the other components.

room temperature. Moreover, our approach differed slightly from that of Brady et al., in that we generated Clausius-Clapeyron functions using point differentiation that allowed us to analyze an effective continuum of data rather than discrete and finite intervals. This introduced an additional source of difference for extrapolated vapor pressure values in our work compared to those data presented in the literature.

Computational approaches to estimating the physical properties of explosives have been realized by Boddu, et al., who calculated vapor pressures using the quantum chemical thermodynamics simulation tool COSMOtherm [24]. The predictions gleaned from these simulations yielded vapor pressures, which were significantly greater than

experimental values. Discrepancies between calculated values and those experimental data found in the literature arise due to a dearth of fundamental physical data regarding these weakly volatile compounds. Computational estimations rely upon accurate physical data such as critical points, acentric factor, and enthalpies of fusion and vaporization [24], all of which have limited or no presence in the experimental literature for new munitions formulations or their components. Thus, COSMOtherm predictions were generated based upon information regarding molecular structure [24]. Therefore, while the absolute value of the predictions for a particular formulation may not be accurate, it has been shown that trends amongst compounds

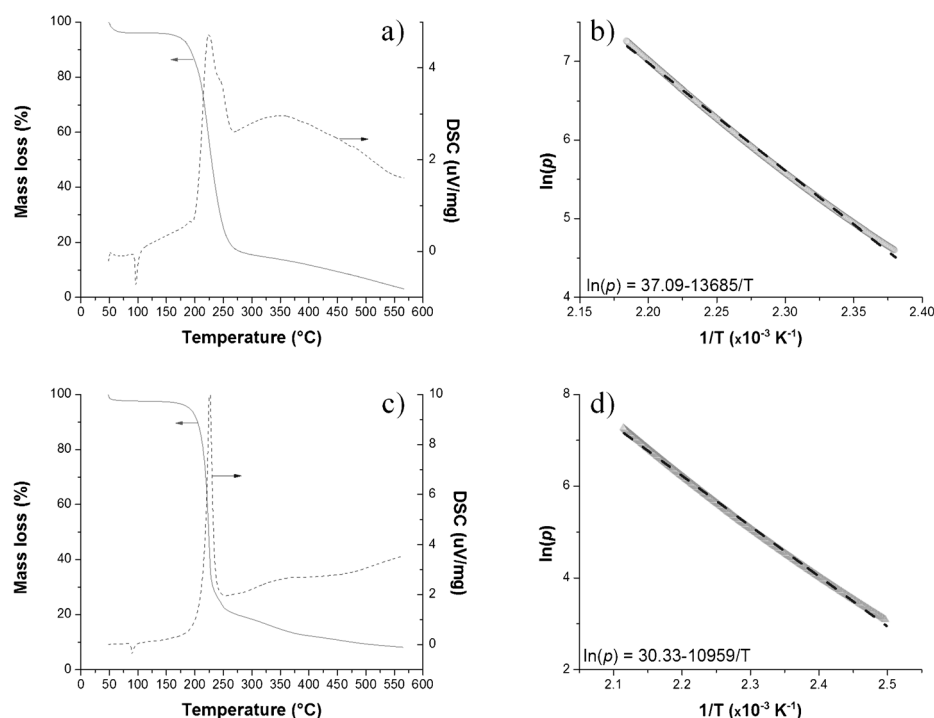


**Figure 3.** TGA/DSC traces for (a) IMX-101 and (c) IMX-104 formulations. Plots of  $\ln(p)$  vs.  $T^{-1}$  for each formulation yield a vapor pressure relationship of (b)  $\ln(p) = 37.1 - 13685/T$  for IMX-101, and (d)  $\ln(p) = 30.3 - 10959/T$  for IMX-104.

**Table 2.** Vapor pressure data for munitions materials calculated from TGA/DSC measurements.

Material	DSC phase transition onset [°C]	Clausius-Clapeyron relation	Applicable $T$ range [°C]	Vapor pressure extrapolated to 298 K [Pa]	$\Delta_{\text{sub}}H$ calculated [kJ mol <sup>-1</sup> ]	$\Delta_{\text{sub}}H$ literature [kJ mol <sup>-1</sup> ]
DNAN (solid)	91	$93.8 - 29884/T$	55–90	$1.53 \times 10^{-3}$	248	243.8 <sup>a)</sup>
DNAN (liquid)	205	$27.1 - 9458/T$	165–250	0.01	—	—
NTO	265	$41.1 - 17709/T$	205–250	$1.10 \times 10^{-8}$	147	98–120 <sup>b)</sup>
NQ	236	$40.6 - 16752/T$	190–225	$1.65 \times 10^{-7}$	139	142.7 <sup>c)</sup>
RDX	210	$43.0 - 17665/T$	170–200	$8.52 \times 10^{-8}$	147	130 <sup>d)</sup>
IMX-101	196	$34.5 - 12625/T$	145–190	$3.84 \times 10^{-4}$	105	—
IMX-104	195	$30.4 - 11007/T$	125–190	$1.45 \times 10^{-3}$	92	—

a) Estimated from  $(\Delta_f H + \Delta_v H)$ , Ref. [12]. b) From Ref. [7]. c) From Ref. [22]. d) From Ref. [8].

do agree with experimental findings. For example, for RDX at  $T = 298$  K, COSMOtherm predicts a vapor pressure of ca.  $10^{-4}$  Pa [24], inconsistent both with the literature results discussed above and our measurements. The value of vapor pressure for RDX extrapolated to room temperature based on our work is  $8.5 \times 10^{-8}$  Pa. However, the trends in vapor pressure for the COSMOtherm predictions nonetheless agree well with our findings, specifically that the rank according to decreasing volatility is: DNAN > RDX > NTO. This suggests that, as experimental capabilities are refined to explore fundamental physical values integral to building computational methods, the accuracy of prediction will increase substantially.

Vapor pressure estimates for IMX formulations were made under the necessary assumption that each formula-

tion intrinsically behaves as a single substance, rather than as several discrete and potentially competing components. For these formulations, Figure 3b and d, the volatility lies just below DNAN for vapor pressures extrapolated to room temperature; this pressure ought to be sufficient to allow vapor detection given recent advances in technology [25]. However, the slopes of the best-fit lines in Figure 3b,d for plots of  $\ln(p)$  vs.  $T^{-1}$  differ slightly for IMX-101 vs. IMX-104, implying there is fundamental difference in enthalpy associated with the sublimation of the solid material.

The Clausius-Clapeyron relationship as applied to vapor pressure of solid materials integrates in the form,

$$\ln(p_i) = c - \frac{\Delta_{\text{sub}}H}{RT} \quad (5)$$

where  $c$  is a constant, and the enthalpy of sublimation,  $\Delta_{\text{sub}}H$ , can be determined from the equations provided in Table 2. Generally, we find good agreement between our calculated values of sublimation enthalpies and those found in the literature. This suggests that the TGA method provides reasonable estimates of  $\Delta_{\text{sub}}H$ . For IMX-101, we calculate  $\Delta_{\text{sub}}H = 105 \text{ kJ mol}^{-1}$ , which compares well with TNT ( $\Delta_{\text{sub}}H = 113 \text{ kJ mol}^{-1}$  [23]), the material that IMX-101 is slated to replace. Notably, IMX-104 ( $\Delta_{\text{sub}}H = 92 \text{ kJ mol}^{-1}$ ), poised to supplant Composition B, does not compare as well with the components of Comp B (RDX and TNT,  $\Delta_{\text{sub}}H = 130$  and  $92 \text{ kJ mol}^{-1}$ , respectively), as measured in this work. However, it is necessary to reiterate that these calculations are made under the assumption that IMX formulations behave a cohesive unit, and as such, our estimated values represent an ideal case.

The fundamental properties associated with IMX formulations provide a foundation for future assessment of the impact of this new class of materials as they are transitioned to the forefront of emerging technologies. In particular, preliminary analyses are useful for anticipatory investigations of fate and toxicity studies and remediation plans as these materials become deployed. Ultimately, vapor pressure and thermodynamic values represent a critical base, upon which to conduct further computational and experimental investigations of these new materials.

## Conclusions

We have demonstrated an extension of the rising temperature TGA technique to determine vapor pressures for new explosives formulations IMX-101 and IMX-104. The technique yields values of vapor pressure and enthalpies of sublimation that are generally in good agreement with established literature values for the discrete components of the IMX formulations, lending confidence to those values determined for IMX-101 and IMX-104. Overall, the vapor pressure of either IMX formulation at  $T = 298 \text{ K}$  is expected to be slightly less than that of the most volatile component, DNAN.

## Acknowledgments

The use of trade, product, or firm names in this report is for descriptive purposes only and does not imply endorsement by the U.S. Government. The tests described and the resulting data presented herein, unless otherwise noted, were obtained from research conducted under the Environmental Quality Technology Program of the United States Army Corps of Engineers by the USAERDC. Permission was granted by the Chief of Engineers to publish this information. The findings of this report are not to be construed as an official Department of the Army position unless so designated by other authorized documents. The authors also wish

to acknowledge Bob Winstead of BAE Systems' Ordnance Systems, Inc. for generously supplying IMX formulations.

## References

- [1] D. Mackay, S. Paterson, Evaluating the Multimedia Fate of Organic Chemicals: A Level III Fugacity Model, *Environ. Sci. Technol.* **1991**, 25, 427.
- [2] H. Östmark, S. Wallin, H. G. Ang, Vapor Pressure of Explosives: A Critical Review, *Propellants Explos. Pyrotech.* **2012**, 37, 12.
- [3] J. W. Grate, R. G. Ewing, D. A. Atkinson, Vapor-Generation Methods for Explosives-Detection Research, *TrAC Trends Anal. Chem.* **2012**, 41, 1.
- [4] R. G. Ewing, M. J. Waltman, D. A. Atkinson, J. W. Grate, P. J. Hotchkiss, The Vapor Pressures of Explosives, *TrAC Trends Anal. Chem.* **2013**, 42, 35.
- [5] W. M. Hikal, J. T. Paden, B. L. Weeks, Rapid Estimation of Thermodynamic Parameters and Vapor Pressures of Volatile Materials at Nanoscale, *ChemPhysChem* **2012**, 13, 2729.
- [6] S. Alnemrat, J. P. Hooper, Predicting Temperature-Dependent Solid Vapor Pressures of Explosives and Related Compounds Using a Quantum Mechanical Continuum Solvation Model, *J. Phys. Chem. A* **2013**, 117, 2035.
- [7] J. E. Brady, J. L. Smith, C. E. Hart, J. Oxley, Estimating Ambient Vapor Pressures of Low Volatility Explosives by Rising-Temperature Thermogravimetry, *Propellants Explos. Pyrotech.* **2012**, 37, 215.
- [8] J. M. Rosen, C. Dickinson, Vapor Pressures and Heats of Sublimation of Some High-Melting Organic Explosives, *J. Chem. Eng. Data* **1969**, 14, 120.
- [9] A. D. Site, The Vapor Pressure of Environmentally Significant Organic Chemicals: A Review of Methods and Data at Ambient Temperature, *J. Phys. Chem. Ref. Data* **1997**, 26, 157.
- [10] S. P. Verevkin, V. N. Emel'yanenko, Transpiration Method: Vapor Pressures and Enthalpies of Vaporization of Some Low-Boiling Esters, *Fluid Phase Equilib.* **2008**, 266, 64.
- [11] J. S. Chickos, Sublimation Vapor Pressures as Evaluated by Correlation-Gas Chromatography, *J. Chem. Eng. Data* **2009**, 55, 1558.
- [12] J. Akhavan, *The Chemistry of Explosives*, Royal Society of Chemistry, Cambridge, UK, **2011**.
- [13] G. T. Long, B. A. Brems, C. A. Wight, Thermal Activation of the High Explosive Nto: Sublimation, Decomposition, and Autocatalysis, *J. Phys. Chem. B* **2002**, 106, 4022.
- [14] Z.-R. Liu, C.-Y. Wu, Y.-H. Kong, C.-M. Yin, J.-J. Xie, Investigation of the Thermal Stability of Nitroguanidine Below Its Melting Point, *Thermochim. Acta* **1989**, 146, 115.
- [15] F. C. Rauch, A. J. Fanelli, Thermal Decomposition Kinetics of Hexahydro-1,3,5-Trinitro-S-Triazine above the Melting Point: Evidence for Both a Gas and Liquid Phase Decomposition, *J. Phys. Chem.* **1969**, 73, 1604.
- [16] I. Langmuir, The Vapor Pressure of Metallic Tungsten, *Phys. Rev.* **1913**, 2, 329.
- [17] G. V. Kunte, U. Ail, P. K. Ajikumar, A. K. Tyagi, S. A. Shivashankar, A. M. Umarji, Estimation of Vapour Pressure and Partial Pressure of Subliming Compounds by Low-Pressure Thermogravimetry, *Bull. Mater. Sci.* **2011**, 34, 1633.
- [18] K. Chatterjee, D. Dollimore, K. Alexander, A New Application for the Antoine Equation in Formulation Development, *Int. J. Pharm.* **2001**, 213, 31.
- [19] J. Elder, Sublimation Measurements of Pharmaceutical Compounds by Isothermal Thermogravimetry, *J. Therm. Anal. Calorim.* **1997**, 49, 897.

- [20] D. R. Stull, Vapor Pressure of Pure Substances. Organic and Inorganic Compounds, *Ind. Eng. Chem.* **1947**, 39, 517.
- [21] G. T. Long, S. Vyazovkin, B. A. Brems, C. A. Wight, Competitive Vaporization and Decomposition of Liquid RDX, *J. Phys. Chem. B* **2000**, 104, 2570.
- [22] R. B. Cundall, T. Frank Palmer, C. E. C. Wood, Vapour Pressure Measurements on Some Organic High Explosives, *J. Chem. Soc. Faraday Trans.* **1978**, 74, 1339.
- [23] B. C. Dionne, D. P. Rounbehler, E. K. Achter, J. R. Hobbs, D. H. Fine, Vapor Pressure of Explosives, *J. Energ. Mater.* **1986**, 4, 447.
- [24] V. M. Boddu, S. W. Maloney, R. K. Toghiani, H. Toghiana, *Prediction of Physicochemical Properties of Energetic Materials for Identification of Treatment Technologies for Waste Streams*, USACE Construction Engineering Research Laboratory Technical Report, **2010**.
- [25] R. G. Ewing, D. A. Atkinson, B. H. Clowers, Direct Real-Time Detection of RDX Vapors under Ambient Conditions, *Anal. Chem.* **2013**, 85, 389.

Received: June 4, 2013

Revised: August 6, 2013

Published online: December 2, 2013